ELSEVIER

Journal of Chromatography A, 697 (1995) 533–540

JOURNAL OF CHROMATOGRAPHY A

Chromatographic separation of continuous mixtures in distributed pores

Benjamin J. McCoy

Department of Chemical Engineering and Materials Science, University of California, Davis, CA 95616, USA

Abstract

Complex multi-component mixtures are conveniently modeled with frequency distribution functions that are continuous functions of a molecular property, e.g., molecular radius. Size-exclusion chromatographic separations can be simulated by accounting for the partitioning of the species in the pores of the stationary phase. The mathematical theory in this paper describes the separation of solutes based on relative sizes of pores and molecules. Linear partition coefficients are represented for continuous distributions of molecular sizes in either continuous or discrete distributions of cylindrical pores. Fractal distributions of pores also illustrate the partitioning behavior. The mass balance equation that governs the frequency distribution of the spherical molecules can be solved exactly when axial dispersion is the only rate process. This equilibrium-dispersive model yields temporal moment expressions that are also useful for interpreting chromatographic data.

1. Introduction

Size-exclusion chromatography (SEC) allows the separation into size fractions of a mixture of different-sized solutes by their partitioning into pores of different radii [1,2]. This defining statement suggests that a complete analysis of SEC requires consideration of the distributions of both solutes and pores. Both discrete and continuous distributions may be contemplated, but many realistic systems will have essentially continuous distributions of both pores and solutes.

Continuous-mixture theories [3,4] of complex multi-component systems are based on the concept of the concentration frequency distribution function (FDF), $C(x)$, which is defined so that the concentration in the property range $(x, x + dx)$ is $C(x)\,dx$. When integrated over the entire range of the property x, the FDF becomes the lumped concentration, c. This approach explains chromatographic separations based on molecular properties of mobile complex mixtures that interact with an immobile phase [5,6]. Goto et al. [7] applied the concept to multi-component leaching or extraction from porous particles in a continuous-flow system. Desorption from the solid matrix and partitioning between the extraction fluid and an immiscible fluid in the pores of the matrix were included.

The earlier works laid a foundation for understanding and extending the approach, but much remains to be done to explore fully the possibilities of this theory. The models for single-sized pores have not yet been extended to the more realistic case of distributed pores. Hence it is the objective of this paper to examine in greater detail the nature of the partitioning of molecules in porous chromatographic media. Specifically, we consider here the effect of a distribution of cylindrical pore sizes on the separation of a

0021-9673/95/$09.50
SSDI 0021-9673(94)01087-0

mixture of distributed spherical molecules. Fractal pore-size distributions illustrate the behavior of the partitioning coefficient for discrete distributions. The combined influences of the single-particle partition coefficient for spheres in cylinders, the distribution of pore sizes and the distribution of spherical molecule sizes yield results of mathematical and practical interest.

2. Chromatographic theory

Assuming that the concentration frequency distribution is $C(x, z, t)$, we can write the total, or lumped, concentration, $c(z, t)$, as the integral over x;

$$c(z, t) = \int_0^\infty C(x, z, t)\, dx \tag{1}$$

The mechanism for size-exclusion separation in chromatography is partitioning of the solutes in pores of the immobile phase. The frequency distribution of the partitioned species can be defined such that the concentration in the interval $(x, x + dx)$ is $Q(x)\, dx$. The lumped partitioned concentration, which is a function of position and time, is the integral

$$q(z, t) = \int_0^\infty Q(x, z, t)\, dx \tag{2}$$

In the present treatment we consider only linear relationships between Q and C, i.e.,

$$Q(x) = K(x)C(x) \tag{3}$$

where for chromatography Q and C will also depend on position z and time t, but $K(x)$ is considered uniform and constant (independent of z and t).

2.1. Equilibrium-dispersive model

In the absence of chemical reactions, the molecular properties of the different chemical species are unchanged. Then the mass balance equations that apply for the concentration also govern the frequency distributions, $C(x, z, t)$ and $Q(x, z, t)$:

$$\varepsilon\, \partial C/\partial t + (1 - \varepsilon)\, \partial Q/\partial t + v\, \partial C/\partial z = D\, \partial^2 C/\partial z^2 \tag{4}$$

in terms of the superficial velocity v, the void fraction ε and the axial dispersion coefficient D. The axial dispersion coefficient, which can be assumed to incorporate other mass transfer resistances, is considered constant.

For an impulse input to the chromatographic column the initial and boundary conditions are

$$C(x, z, t = 0) = 0 \tag{5}$$

$$C(x, z = \infty, t) = 0 \tag{6}$$

$$C(x, z = 0, t) = C_0(x)\, \delta(t)\tau \tag{7}$$

where $\tau = z/v$.

2.2. Exact solution

When the linear adsorption isotherm is Eq. (3), the chromatographic equation can be written as

$$A(x)\, \partial C/\partial t + v\, \partial C/\partial z = D\, \partial^2 C/\partial z^2 \tag{8}$$

where

$$A(x) = \varepsilon + (1 - \varepsilon)K(x) \tag{9}$$

The solution [8,9] that satisfies the initial and boundary conditions is

$$C(x, z, t) = [C_0/(4\pi Dt/Az^2)^{1/2}] \exp[-(1 - vt/Az)^2/(4Dt/Az^2)] \tag{10}$$

which is valid for $t \geq 0$ and $z \geq 0$. The asymptotic solution for $D/vz \to 0$ is

$$C(x, z, t) = [C_0/(4\pi D/vz)^{1/2}] \exp[-(1 - vt/Az)^2/(4D/vz)] \tag{11}$$

which is Gaussian in t.

2.3. Moment solution

When other mass transfer or adsorption rate processes are incorporated into the chromatographic model, an exact solution is usually not feasible. In such cases one can apply moment methods, which provide moment expressions that allow the interpretation of experimental

observations of chromatographic output. Moreover, the moments can be used to construct an approximate solution to the chromatographic equation. We next solve the partial differential Eq. 11 by applying the temporal moment method, which entails computing limits of the derivatives of Laplace transform solutions. The expressions for the moments are readily derived from

$$M_n(x, z) = \lim_{s\to 0} (-1)^n \, \mathrm{d}^n C/\mathrm{d}s^n \tag{12}$$

where $C(x, z, s)$ is the Laplace transform of $C(x, z, t)$. The zero, first and second temporal moments [5] of the frequency distributions, when we use the isotherm Eq. 3, are

$$M_0(x, z) = M_0(x, z = 0) = M_0(x) = C_0(x)A(x)z/v \tag{13}$$

$$M_1(x, z) = M_0(x)A(x)z/v \tag{14}$$

$$M_2(x, z) = M_0(x)[A(x)z/v]^2(1 + D/2v) \tag{15}$$

These moment expressions determine the pulse response for any value of the property x.

The temporal moments of the lumped concentration, $c(z, t)$, according to Eq. 1, are the integrals over x:

$$m_n(z) = \int_0^\infty M_n(x, z)\,\mathrm{d}x \tag{16}$$

where n is the order of the moment, i.e., 0, 1 or 2. The reduced first moment is defined as

$$\mu_1' = m_1/m_0 \tag{17}$$

and the variance as

$$\mu_2 = m_2/m_0 - (\mu_1')^2 \tag{18}$$

The results for the lumped moments are as follows [5]:

$$\mu_1' = \langle A\rangle z/v \tag{19}$$

$$\mu_2 = 2Dz\langle A^2\rangle/v^3 + (z/v)^2[\langle A^2\rangle - \langle A\rangle^2] \tag{20}$$

where

$$\langle A^n\rangle = \int_0^\infty A(x)^n C_0(x)\,\mathrm{d}x \Big/ \int_0^\infty C_0(x)\,\mathrm{d}x \tag{21}$$

is the average over x of the nth power of $A(x)$. If the parameter $K(x)$ has only one value, namely $K_0\,\delta(x - x_0)$, then $\langle A^n\rangle = \langle A\rangle^n$ and the usual moments for a single component system are recovered. However, since in general $\langle A^2\rangle - \langle A\rangle^2 = \langle (A - \langle A\rangle)^2\rangle$, the variance of the lumped concentration of the continuous mixture is greater than the variance of the single-component system. Thus the lumped HETP, defined as $z\mu_2/(\mu_1')^2$, would be greater than that for a single-component system. Expressions for the third moment indicating asymmetry were also discussed by McCoy [5].

To portray the time dependence of the frequency distributions at any position z, one can represent $C(x, z, t)$ as a Gaussian function [10,11]:

$$C(x, z, t) = [M_0/(2\pi\sigma^2)^{1/2}] \times \exp[-(t - M_1/M_0)^2/(2\sigma^2)] \tag{22}$$

where

$$\sigma^2 = M_2/M_0 - (M_1/M_0)^2 \tag{23}$$

is the variance of the frequency distribution. By substituting the moment expressions, Eqs. 13–15, one can show that the moment solution is equivalent to the asymptotic solution, Eq. 11. For relatively long columns, high velocities or small dispersion, the approximate solution is satisfactory.

The HETP for each value of x can be defined as

$$H(x) = z\sigma^2/(M_1/M_0)^2 \tag{24}$$

which yields on substitution of Eqs. 13–15 and 23

$$H(x) = 2D/v \tag{25}$$

The HETP for a continuous mixture that obeys the model of Eq. 8 is thus independent of x unless dispersion and mass transfer provide for $D(x)$.

The chromatographic behavior of a continuous mixture was illustrated for examples of the partition coefficient, $K(x)$, and the feed distribution, $C_0(x)$, in Ref. [6]. The input to the chromatographic column was assumed to be Gaussian:

$$C_0(x) = G\exp[-(x - 2)^2] \tag{26}$$

The partition coefficient, for $x \leq r$, was taken as

$$K(x) = (1 - x/r)^2 \tag{27}$$

thus smaller molecules are more strongly retained than larger molecules. The consequent behavior is reflected in the concentration contours plotted on t versus x, where the contours slope downward to the right [6]. For the linear adsorption isotherm, larger molecules are retained longer in the column, and the contours slope upward.

3. Partitioning in distributed pores

The single-pore partition coefficient accounts for exclusion of the spherical solute from an annular region of the cylindrical pore, or from the pore itself if the sphere is larger than the pore,

$$\Phi(x, r_j) = (1 - x/r_j)^2 \qquad \text{for } x < r_j$$
$$\Phi(x, r_j) = 0 \qquad \text{for } x \geq r_j \tag{28}$$

Consider the case when the pores are not simply of one size, but are distributed in radius according to a given continuous or discrete function. Denote the normalized frequency distributions by n_j and $n(r)$ for discrete and continuous cases, respectively:

$$1 = \sum_j n_j \qquad \text{and} \qquad 1 = \int n(r)\,dr \tag{29}$$

For the discrete distribution the actual partitioned concentration, $Q(x)$, is the sum over all size pores, and we obtain Eq. (3), $Q(x) = K(x)C(x)$, where

$$K(x) = \sum_j n_j \Phi(x, r_j) \tag{30}$$

is the distributed-pore partition coefficient. For the continuous distribution, we have the integral expression for $K(x)$:

$$K(x) = \int n(r)\Phi(x, r)\,dr \tag{31}$$

Thus, when local equilibrium applies for all z and t, we can always write the distribution coefficient as $K(x)$. The discontinuous nature of $\Phi(x, r)$ calls for special attention in the summation or integration to obtain $K(x)$. The dependence of K on x is required to connect the limiting values $K(x = 0) = 1$ (vanishingly small solutes are totally partitioned in the pores), and $K(x \geq r_{max}) = 0$ (solutes larger than the largest pore are totally excluded from the pores).

To illustrate the behavior of a continuous pore-size distribution, we first consider a distribution of single-size pores, $n(r) = \delta(r - r_0)$. When integrated according to Eq. 31 one obtains

$$K(x) = \Phi(x, r_0) \tag{32}$$

which is pictured in Fig. 1 for $r_0 = 1$, 0.5 and 0.1. The maximum value of r is r_0, and as r_0 becomes vanishingly small, $K(x)$ goes to zero since all solutes are excluded from infinitesimally small pores.

Next, consider the normalized rectangular distribution

$$n(r) = 1/(r_2 - r_1) \tag{33a}$$

for $r_1 \leq r \leq r_2$ and

$$n(r) = 0 \tag{33b}$$

otherwise. The partition coefficient $K(x)$ has the three different values depending on the value of x:

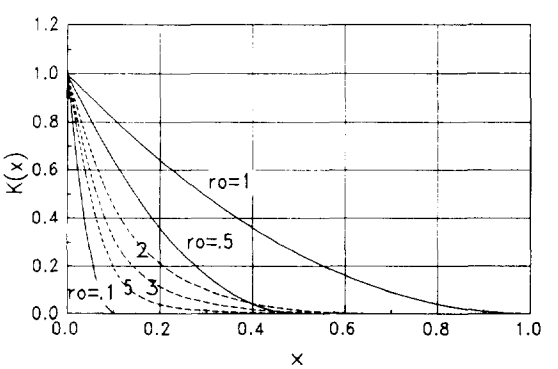

Fig. 1. The distributed-pore partition coefficient, $K(x)$, plotted versus the solute radius, x, for a distribution of single-size pores, $n(r) = \delta(r - r_0)$, with $r_0 = 1$, 0.5, 0.1 (solid lines), and for fractal media with cylindrical pores ($\Omega = \pi$, $\sigma = 1.5$, $a = 1$) and $h = 2$, 3 and 5 (dashed lines).

if $x > r_2$, then $K(x) = 0$

if $x < r_1$, then $K(x) = 1 + 2x \ln(r_1/r_2)/(r_2 - r_1) + x^2/r_1 r_2$

if $r_1 \leq x \leq r_2$,

then $K(x) = 2x \ln(x/r_2)/(r_2 - r_1) + (r_2^2 - x^2)/r_2(r_2 - r_1)$ (34)

$K(x)$ is plotted in Fig. 2, where $r_2 = 1.0$ and $r_1 = 0.5$, and the values at $K(x = r_1)$ match smoothly as required.

A continuous power-law distribution of pore sizes is defined by

$$n(r) = (b + 1)r^b \tag{35}$$

Integrating $n(r)\Phi(x, r)$ over r between x and 1 (i.e., $x \leq r \leq 1$) yields

$$K(x) = 1 - x^{b+1} - 2x(b + 1)(1 - x^b)/b + x^2(1 - x^{b-1})(b + 1)/(b - 1) \tag{36}$$

which is plotted in Fig. 2 for several values of b. As b increases, $K(x)$ approaches $(1 - x)^2$. These pore-size distributions demonstrate cut-off behavior for solutes larger than r_{max}.

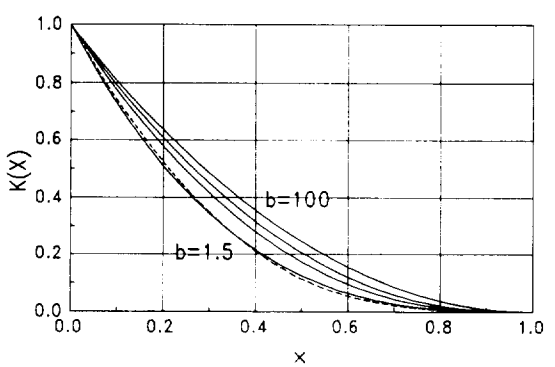

Fig. 2. The distributed-pore partition coefficient, $K(x)$, plotted versus the solute radius, x, for a rectangular distribution of pores (Eq. 33) with $r_1 = 0.5$ and $r_2 = 1.0$ (dashed line), and for a power-law distribution (Eq. 35) with $b = 1.5$, 5 10 and 100 (solid lines).

4. Fractal pore-size distributions

Discrete pore-size distributions can sometimes be represented by a fractal power relationship [12]. A model of a porous membrane with a deterministic fractal distribution of pores can be developed by a conceptual process of making non-intersecting holes of equal length in the immobile phase. Adler [13], in a study of flow in a porous medium, suggested that such fractals could be applied to diffusion and conduction (thermal or electrical), but did not introduce mixtures of different-sized molecules. The benefit of the fractal approach is that simple mathematical equations describe the fractal properties.

We first consider a pore distribution based on the fractal known as the Sierpinski carpet [14], and then generalize the concept to consider holes of different numbers, shapes and sizes. Fig. 3 shows the steps $j = 1, 2, 3$ in the construction of a periodic porous medium from a unit square of area a^2. At step 1 a square hole of edge $a/3$ is formed, and in each of the remaining eight squares a hole of size $(a/3^2)^2$ is formed. This process is repeated indefinitely for every square. The edge length of a square at step j is $r_j = a/3^j$ and its cross-section has area $a^2/9^j$. The number and volume of pores of length L formed at the jth step are

$$n_j = 8^{j-1} \quad \text{and} \quad V_j = L(8/9)^j a^2/8 \tag{37}$$

respectively. The cumulative pore-volume distribution up to the jth step can be shown to be $La^2[1 - (8/9)^j]$, which becomes La^2 if $j \to \infty$, meaning that the volume La^2 is eventually removed by making square holes in the membrane. The discrete pore-volume distribution as the fractal property that it can be represented by a non-integer power, or fractal dimension, D:

$$V_j/La^2 = B^D(r_j/a)^{2-D} \tag{38}$$

where

$$D = \ln 8/\ln 3 \text{ and } B = 8^{-1/D} \tag{39}$$

The fractal pore distribution can be generalized by considering pores of cross-sectional area Ωr_j^2 where $\Omega = 1$ for squares, π for circles or

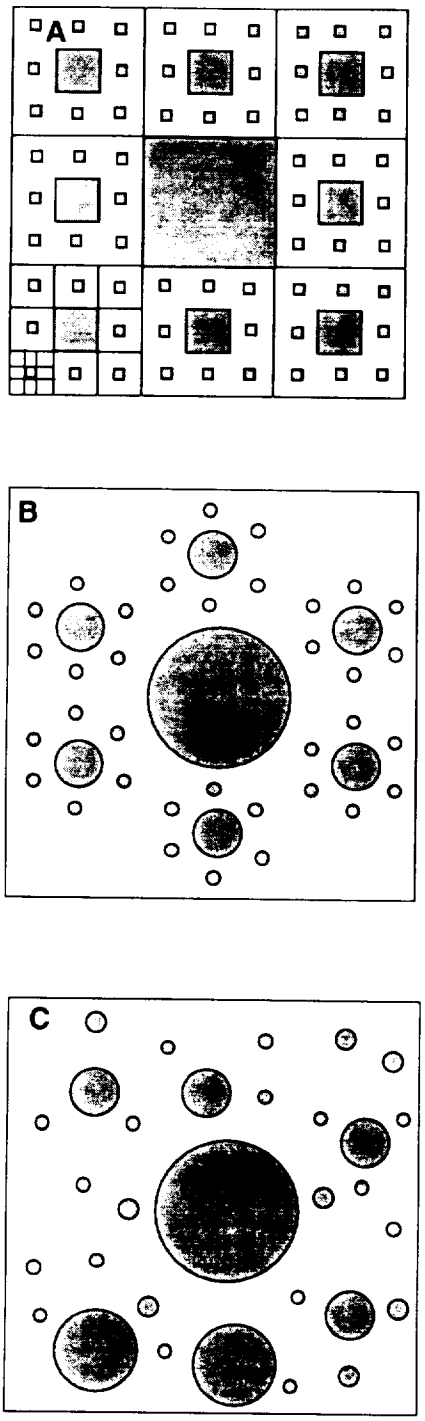

Fig. 3. Steps in the construction of fractal pores in a spatially periodic medium: (A) Sierpinski medium, i.e., $\Omega = 1$, $\sigma = 3$, $h = 8$, $j = 1$–3; (B) $\Omega = \pi$, $\sigma = 3$, $h = 6$, $j = 1$–3; (C) $\Omega = \pi$, $\sigma = 1.5$, $h = 2$, $j = 1$–5.

other constants for other cross-section shapes. Even though the pores are positioned randomly over the solid, the underlying fractal order of pore size applies. The relative size (e.g., radius) of the pores formed at two subsequent steps is defined as the constant σ:

$$\sigma = (\text{size of pore formed at step } j)/(\text{size of pore formed at step } j+1) \quad (40)$$

The relative number of pores formed at subsequent steps is also a constant:

$$h = (\text{number of pores formed at step } j+1)/(\text{number of pores formed at step } j) \quad (41)$$

A similar generalization of the Sierpinski carpet was suggested by Pfeifer and Obert [15]. The size of pores removed at step j is $r_j = a/\sigma^j$, and the volume of a pore is $L\Omega(a/\sigma^j)^2$. The volume removed at the jth step is $L(\Omega a^2/h)(h/\sigma^2)^j$, and the cumulative volume removed is $[L\Omega a^2/(\sigma^2 - h)][1 - (h/\sigma^2)^j]$. When the cumulative volume of pores at the jth step is La^2, the structure possesses fractal properties in a finite range of pore sizes. The fractal dimension D and the premultiplier B in the equation

$$V_j/La^2 = B^D(r_j/a)^{2-D} \quad (42)$$

can be shown to be

$$D = \ln h/\ln \sigma \quad \text{and} \quad B = (\Omega/h)^{1/D} \quad (43)$$

For the Sierpinski pores $\Omega = 1$, $\sigma = 3$ and $h = 8$, and the expressions reduce appropriately to Eqs. 39. If $h = \sigma^2$ then the distribution is rectangular and discrete.

Examples of fractal constructions are pictured in Fig. 3. The Sierpinski carpet (A) shows the first three steps in making the square holes of size ratio $\sigma = 3$ and number ratio $h = 8$. A medium with circular cross-section pores is shown (B) with $\sigma = 3$ and $h = 6$. The random positioning of the pores (C) with $\sigma = 1.5$ and $h = 2$ does not affect the separation process.

Fig. 4 shows the pore volume distribution versus r/a for various values of the parameters. The fractal media display pore-volume distributions that may either increase or decrease with pore size. One may utilize such power-law dis-

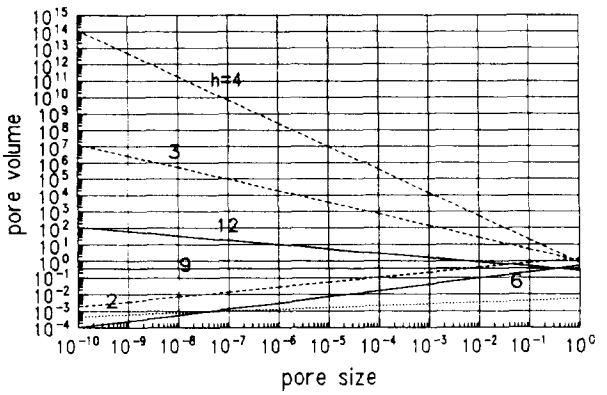

Fig. 4. Log–log plot of the pore-volume distribution: reduced volume, V_j/La^2, versus pore size, r_j/a, for fractal media with cylindrical pores ($\Omega = \pi$), $\sigma = 1.5$ (dashed lines) and $\sigma = 3$ (solid line), and several values of h. The dotted line is the Sierpinski medium ($\Omega = 1$, $\sigma = 3$, $h = 8$).

tributions as continuous distributions. For the discrete distribution, values of r_j are spaced evenly on the logarithmic axis by the amount $\log \sigma$. The line for the square-pore Sierpinski medium would be parallel to the cylindrical-pore case for $\sigma = 3$ and $h = 8$ (not plotted). For a given value of σ, lines for different h intersect at $r = 1/\sigma$.

Table 1 shows values of r_j and $n(r_j)$ for several values of h. If the smallest value of x is 0.1, then $j = 5$ is the smallest pore that will partition the solute. The partition coefficients for these discrete fractal distributions are plotted in Fig. 1. As the largest pore is $r_1 = 0.6667$, $K(x \geq r_1) = 0$ shows the pore cut-off. The partitioning behavior reflected in the integration procedure ensures that $K(x)$ is a continuous function for x in the interval (0, 1). The development of quantitative expressions for temporal moments or contour plots of the concentration frequency distribution is straightforward, and provides the same conclusions summarized above from McCoy [5] and McCoy and Goto [6]. The specific task addressed here, to construct the partition coefficient given a pore-size distribution, provides the essential information needed for the retention time (first moment). Development of expressions showing how the rate processes, e.g., intraparticle diffusion in distributed pores, influence the band broadening (second moment) remains an assignment for the future.

Table 1
Pore size and pore volume fraction in a fractal distribution of five pore sizes ($\sigma = 1.5$, $\Omega = \pi$, $a = 1$)

j	r_j/a	n_j		
		$h = 2$	$h = 3$	$h = 5$
1	0.6667	0.250	0.104	0.023
2	0.4444	0.222	0.138	0.051
3	0.2963	0.197	0.184	0.113
4	0.1975	0.175	0.246	0.252
5	0.1317	0.158	0.328	0.560

5. Conclusions

The distributed-pore partition coefficient, $K(x)$, for a continuous mixture, denoted as a distribution in the solute radius, x, is the key parameter investigated here for size-exclusion chromatography in distributed pores. The function is calculated for continuous and discrete pore distributions. The partitioning of the spherical solute molecules in the cylindrical pores makes use of the single-pore partition factor, $\Phi(x, r)$, to exclude the spherical solute from an annular region of the pore, and to exclude totally solutes larger than a pore. Once $K(x)$ is known, then the exact solution to the equilibrium-dispersive model can be found. Temporal moments can also be computed in order to provide information about how the distribution of solutes is separated in the column. In addition to continuous pore-size distributions, we have examined how fractal distributions of pores can be constructed and integrated to determine $K(x)$. The current theory incorporating size distributions of both solutes and pores thus invites further study of chromatographic and other separation processes involving porous media.

Symbols

$A(x)$ $= \varepsilon + (1 - \varepsilon)K(x)$
$C(x)$ concentration frequency distribution

$C_0(x)$	input concentration frequency distribution
c	lumped concentration
D	axial dispersion coefficient
G	parameter in inlet concentration frequency distribution
HETP	height equivalent to a theoretical plate
$H(x)$	HETP for the concentration frequency distribution
$K(x)$	partition coefficient
$M_0(x)$	zeroth moment of the concentration frequency distribution $C(x)$
$M_1(x)$	first moment of $C(x)$
$M_2(x)$	second moment of $C(x)$
$M_n(x)$	nth moment of $C(x)$
m_n	nth moment of the lumped concentration c
$Q(x)$	concentration frequency distribution of adsorbed species
q	lumped concentration of adsorbed species
t	time
v	superficial column velocity
x	molecular property
z	position coordinate in the chromatographic column

Greek letters

ε	column void fraction
δ	Dirac delta distribution function
μ_1'	$= m_1/m_0$, reduced first moment of the lumped concentration c
μ_2	$= m_2/m_0 - (\mu_1')^2$, variance of the lumped concentration c
σ^2	$= M_2/M_0 - (M_1/M_0)^2$, variance of the frequency distribution

References

[1] R. Tijssen and J. Bos, in F. Dondi and G. Guiochon (Editors), *Theoretical Advancement in Chromatography and Related Separation Techniques* (*NATO ASI Series*, Vol. C383), Kluwer, Dordrecht, 1992.

[2] J.C. Giddings, *Unified Separation Science*, Wiley-Interscience, New York, 1991, pp. 31–35.

[3] G. Astarita and S.I. Sandler (Editors), *Kinetic and Thermodynamic Lumping of Multicomponent Mixtures*, Elsevier, Amsterdam, 1991.

[4] A.V. Sapre and F.J. Krambeck (Editors), *Chemical Reactions in Complex Mixtures*, Van Nostrand Reinhold, New York, 1991.

[5] B.J. McCoy, *Chem. Eng. Sci.*, 44 (1989) 993.

[6] B.J. McCoy and M. Goto, *Chem. Eng. Sci.*, 49 (1994) 2351.

[7] M. Goto, T. Hirose and B.J. McCoy, *J. Supercrit. Fluids*, 7 (1994) 61.

[8] O. Levenspiel and W.K. Smith, *Chem. Eng. Sci.*, 6 (1957) 227.

[9] S. Golshan-Shirazi and G. Guiochon, in F. Dondi and G. Guiochon (Editors), *Theoretical Advancement in Chromatography and Related Separation Techniques*, (*NATO ASI Series*, Vol. C383), Kluwer, Dordrecht, 1992, p. 61.

[10] E. Kucera, *J. Chromatogr.*, 19 (1965) 237.

[11] R.V. Mehta, R.L. Merson and B.J. McCoy, *J. Chromatogr.*, 88 (1974) 1.

[12] P.M. Adler, *Porous Media–Geometry and Transport*, Butterworth-Heinemann, Boston, 1992.

[13] P.M. Adler, in D. Avnir (Editor), *The Fractal Approach to Heterogeneous Chemistry*, Wiley,Chichester, 1989, p. 341.

[14] B.B. Mandelbrot, *The Fractal Geometry of Nature*, Freeman, San Francisco, 1977.

[15] P. Pfeifer and M. Obert, in D. Avnir (Editor), *The Fractal Approach to Heterogeneous Chemistry*, Wiley, Chichester, 1989, p. 35.